JOURNAL OF AGRICULTURAL AND FOOD CHEMISTRY

ARTICLE

pubs.acs.org/JAFC

Influence of Pyrolysis Temperature on Biochar Property and Function as a Heavy Metal Sorbent in Soil

Minori Uchimiya,* Lynda H. Wartelle, K. Thomas Klasson, Chanel A. Fortier, and Isabel M. Lima

USDA-ARS Southern Regional Research Center, 1100 Robert E. Lee Boulevard, New Orleans, Louisiana 70124, United States

Supporting Information

ABSTRACT: While a large-scale soil amendment of biochars continues to receive interest for enhancing crop yields and to remediate contaminated sites, systematic study is lacking in how biochar properties translate into purported functions such as heavy metal sequestration. In this study, cottonseed hulls were pyrolyzed at five temperatures (200, 350, 500, 650, and 800 °C) and characterized for the yield, moisture, ash, volatile matter, and fixed carbon contents, elemental composition (CHNSO), BET surface area, pH, pH_{pzc}, and by ATR-FTIR. The characterization results were compared with the literature values for additional source materials: grass, wood, pine needle, and broiler litter-derived biochars with and without post-treatments. At respective pyrolysis temperatures, cottonseed hull chars had ash content in between grass and wood chars, and significantly lower BET surface area in comparison to other plant source materials considered. The N:C ratio reached a maximum between 300 and 400 °C for all biomass sources considered, while the following trend in N:C ratio was maintained at each pyrolysis temperature: wood ≪ cottonseed hull ≈ grass ≈ pine needle ≪ broiler litter. To examine how biochar properties translate into its function as a heavy metal (Ni^{II}, Cu^{II}, Pb^{II}, and Cd^{II}) sorbent, a soil amendment study was conducted for acidic sandy loam Norfolk soil previously shown to have low heavy metal retention capacity. The results suggest that the properties attributable to the surface functional groups of biochars (volatile matter and oxygen contents and pH_{pzc}) control the heavy metal sequestration ability in Norfolk soil, and biochar selection for soil amendment must be made case-by-case based on the biochar characteristics, soil property, and the target function.

KEYWORDS: biochar, cottonseed hull, pyrolysis, heavy metal, soil

INTRODUCTION

Char is a form of environmental black carbon (BC), a ubiquitous carbonaceous geosorbent in soils and sediments.[1] Because of their widespread existence in high quantity (up to 35% of total organic carbon in soil),[2] extensive studies have been conducted to quantify and distinguish char from other BC components such as soot[3] in environmental samples. In recent years, soil amendment of char products (biochar) from thermochemical processing (slow/fast pyrolysis and gasification) of biomass for biofuel production purposes[4] has received considerable interests. Systematic investigation is necessary to understand how biochar properties translate into purported functions such as contaminant sorption,[1] soil fertilization,[5] and for the use as a fuel.

Antal and co-workers[6,7] provided comprehensive reviews on how feedstock and pyrolysis conditions translate into the structure and properties of char. For example, substances that are rich in oxygen and poor in hydrogen, such as sugar, are nongraphitizing and develop a strong system of cross-linkage that immobilize the structure and unite the crystallites in a rigid mass.[8] Sugars form liquid phases during pyrolysis, and the resulting char does not retain the original physical structure visually, and does not have high porosity.[8] Sucrose-derived chars have no homogeneous development of true graphitic structure even after heating at 3000 °C.[8] Biomass is composed primarily of carbohydrate and lignin and is graphitizing because of the existence of nearly parallel structural units held together with a small number of weak cross-linkages. Carbonization involves the growth of aromatic structure and polymerization resulting in carbon enrichment and development of porosity as volatile matter is removed. In addition, ash (e.g., K_2O, P_2O_5, MgO, Na_2O) may catalyze graphitization and oxidation processes during pyrolysis.[8]

More recently, Keiluweit et al.[9] employed synchrotron-based near-edge X-ray absorption fine structure spectroscopy (NEXAFS) and X-ray diffraction (XRD) to demonstrate how grass (lignin-poor) and wood (lignin-rich) undergo analogous but quantitatively different transformation during slow pyrolysis at 100−700 °C.[9] The following temperature-dependent structural transition was proposed: (1) transition char having crystalline character of the precursor materials preserved, (2) amorphous char that is a random mixture of thermally altered molecules and incipient aromatic polycondensates, (3) composite chars having poorly ordered graphene stacks embedded in amorphous phases, and (4) turbostratic char dominated by disordered graphitic crystallites.[9] Abrupt changes in crystallinity and porosity as well as the loss of oxygen and hydrogen occurred at 300−500 °C, and volatile matter (VM) decreased (and fixed carbon increased) most substantially at 400−600 °C. Chars formed at higher temperatures (lower oxygen to carbon ratio)

Received: October 28, 2010
Revised: January 28, 2011
Accepted: January 31, 2011
Published: February 24, 2011

are expected to be π donor, while chars formed at lower temperatures are expected to be π acceptor.[10]

A number of studies have been conducted to determine how structural changes as a function of pyrolysis temperature translate into the function of char as the sorbent for organic compounds such as naphthalene, nitrobenzene, *m*-dinitrobenzene,[11] benzene,[12] and catechol.[13] Gradual transition in sorption mechanism was observed from partitioning into the residual (noncarbonized) organic fractions to adsorption on carbonized fractions as a function of pyrolysis temperature.[11] To our knowledge, systematic study is currently nonexistent on how pyrolysis temperature and resulting char property translate into their function as the heavy metal sorbent in soils. Heavy metal sequestration is an important target function of biochars for both soil fertilization and environmental remediation purposes. In this study, biochars were produced at five pyrolysis temperatures (200, 350, 500, 650, and 800 °C) and, after rigorous characterization (yield, moisture, ash, VM, fixed C, elemental composition, ATR-FTIR, BET surface area, pH, and pH_{pzc}), screened for the ability to sequester Ni^{II}, Cu^{II}, Pb^{II}, and Cd^{II} in acidic sandy loam Norfolk soil that showed low capacity for retaining copper in our previous study.[14] Heterogeneous nature of cottonseed hull (containing both hulls and seeds) resulted in biochars with ash content between grass and wood chars, similar VM and fixed carbon contents as grass chars, and lower BET surface areas relative to grass and wood chars. The results suggest the governing roles of surface functional groups (VM, pH_{pzc}, and O:C and N:C ratios) and minor influence of BET surface area, fixed carbon and ash contents for the heavy metal sequestration ability of biochars on the soil type employed.

MATERIALS AND METHODS

Chemicals. Distilled, deionized water (DDW) with a resistivity of 18 MΩ cm (Millipore, Milford, MA) was used for all procedures. Nickel(II) nitrate, copper(II) chloride dihydrate, lead(II) nitrate, and cadmium(II) nitrate tetrahydrate were purchased from Sigma-Aldrich (Milwaukee, WI), and stock solutions (0.2 M) were prepared in DDW.

Preparation of Biochars. Cottonseed hulls (CH25) were obtained from Planters Cotton Oil Mill (Pine Bluff, AK) and were used as received without pretreatments as a mixture of hulls and cottonseeds. Cottonseed hulls were pyrolyzed at 200, 350, 500, 650, and 800 °C for 4 h under 1600 mL min^{-1} nitrogen flow rate using a box furnace (22 L void volume) with retort (Lindberg, Type 51662-HR, Watertown, WI). The resulting chars (CH200, CH350, CH500, CH650, and CH800) were allowed to cool to room temperature overnight in the retort under 1600 mL min^{-1} nitrogen flow rate.

Additional Carbonaceous Materials Examined. Preparation of broiler litter biochars was described in a previous report.[15] Briefly, broiler litter samples (25BL) were milled (<25% moisture content), pelletized, and pyrolyzed at 350 or 700 °C for 1 h under 1600 mL min^{-1} nitrogen flow rate to form 350BL and 700BL. Activated analogues of 350BL and 700BL (350ABL and 700ABL, respectively) were prepared by steam activation at 800 °C for 45 min under nitrogen atmosphere with 3 mL min^{-1} water flow rate, following the pyrolysis step. To remove excess ash, 350BL, 700BL, 350ABL, and 700ABL were washed with 0.1 M HCl (27 g char L^{-1}) by constant stirring for 1 h, rinsed three times with DDW, dried overnight at 80 °C, and then ground and sieved to less than 44 μm (325 mesh).

Of 350BL, 700BL, 350ABL and 700ABL, 350BL contained the greatest proportion of the noncarbonized fraction.[16] Selected portion of 350BL was further post-treated by base-extraction of the organic fraction[17] by (1) shaking char suspension (9.5 g L^{-1}) end-over-end at 85 rpm in 0.1 M NaOH for 24 h, (2) washing three times with DDW by discarding supernatant after centrifugation at 10,000 rpm for 10 min at 20 °C, and (3) drying for 24 h at 65 °C. The resulting char is hereby termed "base-350BL".

Preparation of phosphoric acid activated carbon from pecan shells was described in a previous report.[18] Briefly, pecan shells were ground and sieved, soaked in 30 wt % phosphoric acid overnight, and heated at 450 °C for 4 h under 800 mL min^{-1} air flow rate. The resulting activated carbon (PS800) was washed five times in hot water (90 °C), oven-dried overnight at 80 °C, and ground and sieved to less than 44 μm. Heavy metal sequestration capacity of 350BL, 700BL, 350ABL, 700ABL, base-350BL, and PS800 in soil has been examined previously.[19]

Surface Area and Elemental Composition. Surface areas were measured in duplicate by nitrogen adsorption isotherms at 77 K using NOVA 2000 surface area analyzer (Quantachrome, Boynton Beach, FL). Specific surface areas were determined from adsorption isotherms using BET equation. The micropore area was calculated using t-plots derived from the NOVA 2000 software. Elemental composition (CHNSO) was determined by dry combustion using Perkin-Elmer 2400 Series II CHNS/O analyzer (Perkin-Elmer, Shelton, CT).

Proximate Analysis. Moisture, ash, volatile matter, and fixed carbon contents of biochars were determined by following American Society for Testing and Materials (ASTM) method D5142[20] using LECO thermogravimetric analyzer (TGA701, LECO, St. Joseph, MI). Proximate analyses were performed in duplicate for each sample. Moisture was determined as the weight loss after heating the char in an open crucible to 107 °C and holding at this temperature until sample weight stabilized. Volatile matter was determined as the weight loss after heating the char in a covered crucible to 950 °C and holding for 7 min. Ash was defined as the remaining mass after subsequently heating in an open crucible to 750 °C and holding at this temperature until sample weight stabilized. After the determination of moisture, ash, and volatile matter, fixed carbon was calculated by difference. Results of proximate analyses are provided as the sample weight and crucible temperature as a function of time in Figure S1, Supporting Information.

ATR-FTIR. Fourier transform infrared (FTIR) spectra were obtained using Bruker Vertex 70 spectrometer (Bruker Optics, Billerica, MA) fitted with a Pike Technologies MIRacle attenuated total reflectance (ATR) accessory (Madison, WI) with a diamond crystal plate. The spectra were obtained at 8 cm^{-1} resolution from 650 to 4500 cm^{-1} with 128 scans. Prior to FTIR analyses, all samples were adjusted to pH 3.0 and dried overnight at 70 °C.

Point of Zero Charge. Prior to the analysis, all cottonseed hull biochars were washed with 0.1 M HCl (27 g char L^{-1}) by constant stirring for 1 h to remove ash, rinsed three times with DDW, dried overnight at 80 °C, and then ground and sieved to less than 44 μm. The point of zero charge (pH_{pzc}) for CH200, CH350, CH500, CH650, and CH800 was determined by a previously described pH drift method.[21,22] Briefly, 5 mM $CaCl_2$ solution was boiled to remove CO_2 and cooled to room temperature. Char sample (0.06 g) was added to 20 mL of the resulting $CaCl_2$ solution preadjusted to pH 4, 6, 8, and 10 using 0.5 M HCl or NaOH, and equilibrated for 24 h by constant stirring in capped glass vials prior to pH measurements. The pH_{pzc} of char was determined as the pH at which the initial pH equals the final pH.[21,22] The results of pH_{pzc} measurements are presented in Figure S2, Supporting Information.

Retention of Pb, Cu, Ni, and Cd in Norfolk Soil. Acid washed cottonseed hull chars (used for the determination of pH_{pzc}) were employed in soil amendment studies. All experiments were conducted using synthetic rainwater (SRW) to simulate contaminant leaching by percolating rainfall.[23] The SRW was prepared daily by adding 10 mM H_2SO_4 to DDW until pH 4.5 was attained.[24] Norfolk loamy sand[25] was obtained from USDA-ARS Coastal Plains Soil, Water and Plant Research Center (Florence, SC) and was air-dried and sieved (2 mm) prior to use. Separate amber glass batch reactors were prepared for Norfolk

Table 1. Yield and Moisture, Volatile Matter (VM), Fixed Carbon and Ash Contents, pH, and pH_{pzc} of Cottonseed Hull Chars[a]

char	yield,[b] % (w/w)	moisture, % (w/w)	VM,[c] % (w/w)	fixed C,[d] % (w/w)	ash,[c] % (w/w)	0.1 M HCl washing, % wt loss[e]	pH[e]	pH_{pzc}
CH200	83.4 ± 0.8	5.3 ± 0.2	69.3 ± 0.2	22.3 ± 0.1	3.1 ± 0.1	4.3	3.7	3.5
CH350	36.8 ± 0.1	6.81 ± 0.01	34.9 ± 0.1	52.6 ± 0.2	5.7 ± 0.1	6.6	6.9	7.0
CH500	28.9 ± 0.1	6.53 ± 0.01	18.6 ± 0.6	67.0 ± 0.7	7.9 ± 0.1	5.7	8.5	10.1
CH650	25.4 ± 0.2	8.21 ± 0.02	13.27 ± 0.04	70.3 ± 0.2	8.3 ± 0.2	9.7	8.6	9.9
CH800	24.2 ± 0.6	9.92 ± 0.05	11.42 ± 0.1	69.49 ± 0.01	9.2 ± 0.1	8.6	7.7	9.2

[a] Proximate analysis results are given as mean ± standard deviation for duplicate measurements. [b] Mean ± SD for replicate production. [c] Moisture-free values. [d] Calculated by difference after moisture, VM, and ash measurements. [e] After 0.1 M HCl washing.

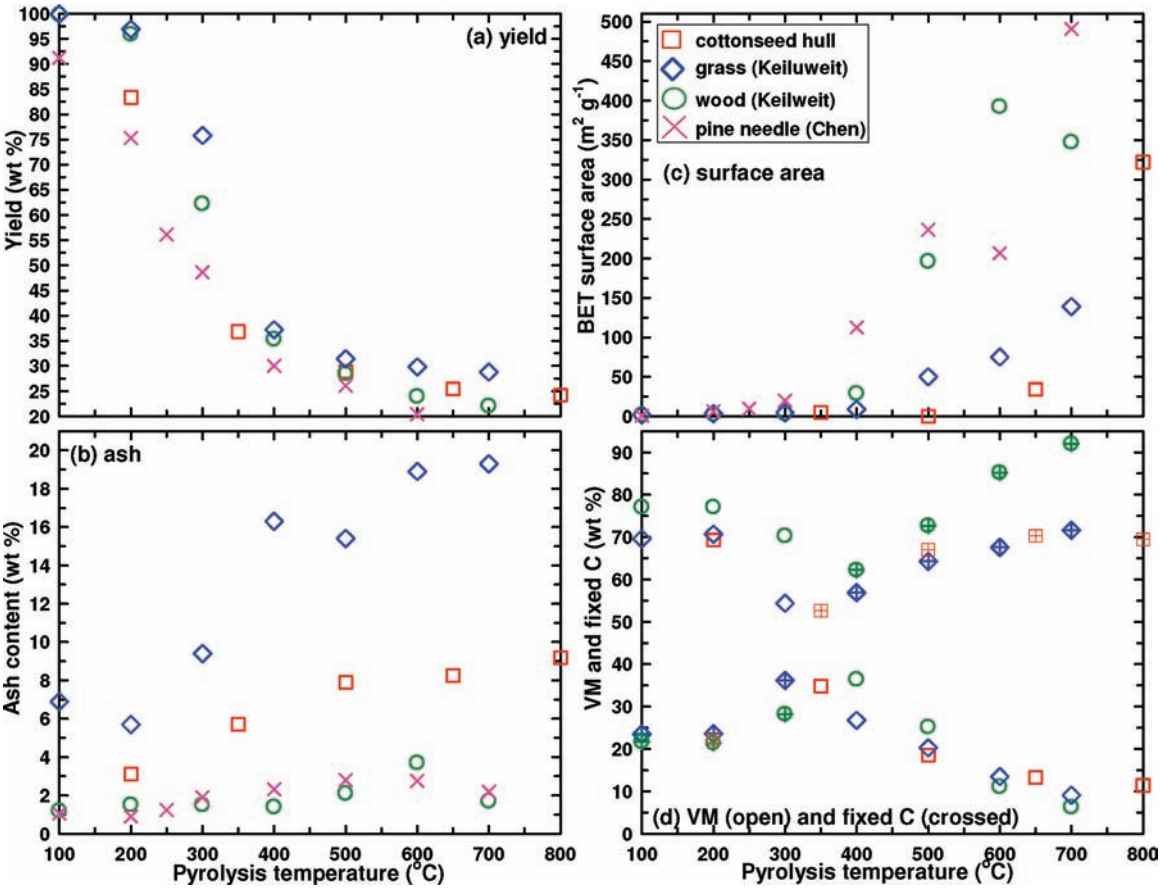

Figure 1. Yield and ash, VM (open points), and fixed C (crossed points) contents, and BET surface area for biochars derived from cottonseed hull and other biomass sources. Grass and wood results were obtained from ref 9, and pine needle results were obtained from ref 11.

soil in SRW (20 g soil L^{-1}) with and without 10% (g biochar g^{-1} soil) CH350, CH500, CH650, CH800, PS800 and 700BL. Total volume of each reactor was set to 20 mL. Selected loading (10 wt %) corresponds approximately to 130 t ha^{-1} (assuming 10 cm soil depth) and is within the range employed in previous biochar amendment studies.[26] Reactors were pre-equilibrated for 48 h by shaking end-over-end at 70 rpm.

After pH measurement (pHt_0; Orion 3-star plus benchtop pH meter, ThermoScientific, Waltham, MA), Pb^{II}, Cd^{II}, Cu^{II}, and Ni^{II} were added together to each reactor for the final concentration of 300 μM for each metal (i.e., each reactor contained 1.2 mM total added metals at t_0). Reactors were equilibrated for 48 h and, following pH measurement (pHt_{48}), filtered (0.2 μm Millipore Millex-GS; Millipore, Billerica, MA). Filtrate was acidified to 4% (v/v) nitric acid (trace metal grade, Sigma-Aldrich) for the determination of soluble Cu, Ni, Cd, and Pb concentrations using an inductively coupled plasma optical emissions spectrometer (ICP-AES; Profile Plus, Teledyne/Leeman Laboratories, Hudson, NH). Each sorption experiment was performed in duplicate.

RESULTS AND DISCUSSION

Biochar Characterization. Table 1 provides the yield and moisture, volatile matter, fixed carbon, and ash contents of cottonseed hull-derived biochars. The biochar yield is reported as mean ± SD for the replicate production using two identical box furnaces. The biochar yield showed an initial rapid decrease followed by a more steady decrease, as a function of pyrolysis temperature (Table 1). The proximate analysis results are reported as mean ± SD for two replicate measurements, and increases in the moisture, fixed carbon, and ash contents and a decrease in volatile matter content were observed as a function of

Table 2. Elemental Composition,[a] Molar Ratio, and BET Surface Area[b] for Cottonseed Hull Chars and Additional Carbonaceous Materials. Values are given as mean ± standard deviation for triplicate (elemental composition) or duplicate (BET surface area) measurements. Elemental composition and molar ratio are given on a moisture- and ash-free basis

char	C, % (w/w)	H, % (w/w)	N, % (w/w)	S, % (w/w)	O, % (w/w)	H/C, molar ratio	O/C, molar ratio	BET SA, $m^2\ g^{-1}$	micropore area, $m^2\ g^{-1}$
CH25	51 ± 2	6.6 ± 0.3	0.7 ± 0.1	1.03 ± 0.05	41 ± 2	1.5 ± 0.1	0.6 ± 0.1	n.d.	
CH200	51.9 ± 0.5	6.0 ± 0.1	0.60 ± 0.04	0.99 ± 0.01	40.5 ± 0.4	1.38 ± 0.02	0.59 ± 0.01	n.d.	
CH350	77 ± 1	4.53 ± 0.05	1.9 ± 0.4	0.8 ± 0.1	15.70 ± 0.04	0.70 ± 0.01	0.153 ± 0.001	4.7 ± 0.8	
CH500	87.5 ± 0.1	2.82 ± 0.02	1.5 ± 0.1	0.50 ± 0.01	7.6 ± 0.2	0.385 ± 0.003	0.065 ± 0.002	0	
CH650	91.0 ± 0.4	1.26 ± 0.02	1.6 ± 0.1	0.26 ± 0.03	5.9 ± 0.3	0.166 ± 0.002	0.049 ± 0.003	34 ± 3	0.007 ± 0
CH800	90 ± 1	0.6 ± 0.1	1.9 ± 0.1	0.16 ± 0.03	7 ± 1	0.08 ± 0.01	0.06 ± 0.01	322 ± 1	274 ± 1
PS800	68 ± 1	3.1 ± 0.1	1.00 ± 0.04	0.48 ± 0.02	27 ± 1	0.55 ± 0.02	0.30 ± 0.01	864	788
25BL	45 ± 1	6.9 ± 0.2	7 ± 2	1.7 ± 0.2	40 ± 1	1.85 ± 0.01	0.67 ± 0.01		
350BL	62.3 ± 0.1	5.53 ± 0.04	6.1 ± 0.1	1.0 ± 0.2	25.0 ± 0.1	1.06 ± 0.01	0.301 ± 0.001	60 ± 20	0
700BL	79 ± 1	2.4 ± 0.1	4.8 ± 0.1	1.6 ± 0.1	13 ± 1	0.37 ± 0.01	0.12 ± 0.01	94 ± 5	42 ± 2
350ABL	68 ± 1	2.6 ± 0.2	4.17 ± 0.05	1.4 ± 0.3	23 ± 1	0.45 ± 0.03	0.26 ± 0.01	335 ± 7	277 ± 5
700ABL	67 ± 1	2.62 ± 0.03	4.0 ± 0.1	1.9 ± 0.2	25 ± 1	0.47 ± 0.01	0.28 ± 0.02	335 ± 1	278 ± 4
base-350BL	56 ± 3	4.9 ± 0.3	18 ± 5	0.82 ± 0.05	20 ± 2	1.05 ± 0.01	0.27 ± 0.02		

[a] Except for oxygen, elemental compositions for PS800 and broiler litter biochars were obtained from ref 19 and converted to moisture- and ash-free values. [b] BET results were obtained from ref 18 for PS800 and ref 16 for broiler litter biochars.

pyrolysis temperature (Table 1). Figure 1 compares results presented in Table 1 (squares) with biochars prepared from other biomass sources under oxygen-limiting conditions: pine wood shavings (*Pinus ponderosa*), tall fescue grass (*Festuca arundinacea*),[9] and pine needles.[11] Grass (diamonds) and wood (circles) chars were produced by heating for 1 h in a muffle furnace.[9] Pine needle chars (crosses) were produced by heating for 6 h in a covered ceramic pot.[11]

For all biomass sources considered in Figure 1a, the yield rapidly decreased from nearly 100% to 30% between 200 and 400 °C and stabilized thereafter, and the lowest yield was observed for the pine needle at respective pyrolysis temperatures. While higher char yield is expected for feedstock high in lignin contents (over cellulose and hemicellulose), the yield strongly depends upon the vapor-phase conditions during pyrolysis.[6]

As reported previously,[9] ash content (Figure 1b) was the highest for grass chars and reached nearly 20% by 700 °C. Ash contents for wood and pine needle chars nearly overlapped and remained low (2−4%) across the temperature range in Figure 1b. The ash contents of cottonseed hull chars are in between the grass and wood/pine needle chars. Ash contents for chars formed by pyrolysis of additional biomass sources at 525 and 650 °C[27] showed similar groupings for the grass and hardwood. That is, the ash content was significantly higher for chars derived from grass (mixed stems and blades of live Eastern gamma grass *Tripsacum dactyloides*; 25% at 525 °C and 16% at 650 °C) than hardwoods (≤1% at 525−650 °C): Loblolly pine (*Pinus taeda*), Eastern red cedar (*Juniperus virginiana*), and tropical hardwood bubinga (*Guibourtia demeusei*).[27] An exception is sugar cane baggase chars that had ash contents (9% at 525 °C and 7% at 650 °C)[27] close in range as cottonseed hull chars (Figure 1b). The ash content of char depends on that of feedstock.[8] For example, oak wood contains little ash, while rice hulls contain a much greater amount of ash in the form of silica.[28] Ash contents of cottonseed hull chars are in agreement with the weight loss after washing with 0.1 M HCl (Table 1).

The volatile matter (VM, open points) and fixed carbon (crossed points) contents of cottonseed hull chars (squares)

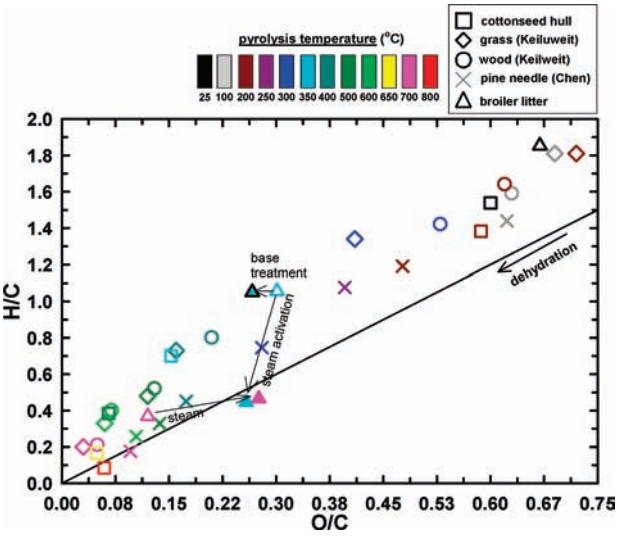

Figure 2. The van Krevelen plot of elemental ratios for chars formed from various biomass sources with and without post-treatments. Thick line represents the direction for dehydration reaction. Pyrolysis temperature is color coded. Filled points are 350ABL and 700ABL. Filled cyan point with black edge is base-350BL.

nearly overlapped with grass chars (diamonds) across the pyrolysis temperature ranges considered in Figure 1d. At ≤400 °C, volatile matter content of hardwood char (open circles, Figure 1d) was significantly greater than that of the cottonseed hull (open squares) or grass (open diamonds) chars. At ≥400 °C, fixed carbon content (crossed points) of hardwood char was significantly greater than that of the cottonseed hull and grass chars. Between 250 and 400 °C, char yield is limited by the formation of "tarry vapor containing a complex soup of organic compounds mixed with noncondensable gases (including CO_2, CO, H_2, CH_4, and heavier hydrocarbons)"[6] that shifts the equilibrium away from char formation. Thermogravimetric analysis of chars at 100−1000 °C showed evolution of water and CO_2 at lower temperatures

and H_2, CH_4, and CO at higher temperatures.[8] Chars containing high VM released aldehyde and other oxygen containing aliphatic compounds as well as aromatic (toluene, phenol, benzene) and carbohydrate decomposition products.[8] Evolution of furan and its derivatives peaked at 360 °C.[8] Antal and Gronli[6] noted that high quality charcoal for use as fuel typically contains 20−30% VM for domestic cooking and is low in ash (0.5−5%).

Table 2 provides the elemental composition and BET surface area of cottonseed hull chars. Elemental composition and molar ratio are given on a moisture- and ash-free basis. Appreciable BET surface areas were obtained only at the highest pyrolysis temperatures (650−800 °C, Table 2). The surface areas of cottonseed hull chars are significantly lower at respective pyrolysis temperatures than the wood, pine needle, or grass chars (Figure 1c). Higher surface areas of hardwood chars, relative to grass chars, have been reported previously.[9] Cottonseed hull chars contain less ash than grass chars (Figure 1b) while the VM contents are similar for the two biomass sources (Figure 1d). Lower BET surface area of cottonseed hull chars likely resulted from additional factors such as the lower H/C ratio (25−200 °C in Table 2) relative to grass and hardwood (100−200 °C in Figure 2). Oxygen-rich and hydrogen-poor substances are less graphitizing due to the formation of extensive cross-linkages during pyrolysis.[7]

In addition to the feedstock, pyrolysis conditions (temperature, gas flow, and the presence of air) impact the surface area of chars, and maximum surface area is typically observed at 500−900 °C.[6] Lower surface area results from lack of atomic size pores within hexagonal carbon layers and pore blockage by VM.[7] As widely discussed, low BET surface area of biochar (Table 2) suggests that the surface area arises primarily from micropores (<1 nm) rather than nanopores (>1 nm)[13] and CO_2 isotherms may be more suitable for detecting the microporosity of char.[29]

The van Krevelen diagram (molar ratios of H:C versus O:C) has been widely employed to deduce the structure and structural changes of complex macromolecules such as humic and fulvic acids,[30] coal, and petroleum crude oil.[31] The van Krevelen diagram has also been utilized to distinguish soot and char components of environmental black carbon[3] and to understand structural transformations during biochar formation.[9] Characteristic lines on the van Krevelen diagram provide an estimate for reaction pathways such as methylation/demethylation, hydrogenation/dehydrogenation, hydration/dehydration, oxidation/reduction, and decarboxylation.[32] Molar ratios of elements have been used to estimate the aromaticity (H:C) and polarity (O:C, (O + N):C, and (O + N + S):C) of chars resulting from the removal of polar surface functional groups and the formation of aromatic structures by higher degree of carbonization of the organic source material during pyrolysis.[11,12]

Figure 2 provides the van Krevelen plot of elemental ratios (all values are given on a moisture- and ash-free basis) for cottonseed hull and additional chars compared in Figure 1. As reported previously for grass and wood chars,[9] all biomass sources followed the line corresponding to dehydration reaction[32] (loss of H_2O indicated by the line having slope of 2 in Figure 2) as a function of pyrolysis temperature up to 800 °C. With increasing pyrolysis temperature, plant biomass undergoes dehydration and depolymerization to form volatile dissociation products of lignin and cellulose and condensation to form graphitic structures.[9] At 200 °C and below, only pine needle followed the dehydration line (Figure 2). For grass and wood, an increase in pyrolysis temperature from 100 to 200 °C did not alter the position (wood) on the van Krevelen diagram or resulted in a slight shift to the right (grass). For cottonseed hulls, pyrolysis at 200 °C led to a nearly vertical downward shift relative to the source material (Figure 2). The greatest shift along the dehydration line occurred at 300−500 °C, and pine needle was closer to the dehydration line than grass, wood, or cottonseed hull. By 600−700 °C, pine needle (600 and 700 °C), cottonseed hull (650 and 800 °C), wood (700 °C), and grass (700 °C) reached the approximate elemental ratios of soot.[3]

Previous studies showed that the van Krevelen diagram allows differentiation of char from a more condensed and aromatic substance, soot.[3] While total carbon contents of soot, char, coal and melanoidin are similar, soot has lower H:C and O:C ratios than char with more condensed graphitic structure and is less prone to oxidation.[3] Soot is formed at 500−800 °C in gas phase as a cluster of micrometer sized spheres and is composed of more than 90% carbon.[3]

Interestingly, except for the pine needle char at 300 °C, only broiler litter steam activated carbons fell within the previously reported approximate elemental ratios of char.[3] Chars formed at 400−600 °C in Figure 2 has lower O:C ratios than the literature values[3] for the elemental ratios of char. As widely described in previous reports,[33] char exists within the "environmental black carbon continuum" that ranges from the highest (biomass) to the lowest (highly condensed aromatic structures) O:C and H:C ratios. Of the source materials considered in Figure 2 (black points denoted 25 °C pyrolysis temperature), both cottonseed hull and broiler litter are close to the literature values of carbohydrate.[3] Cottonseed hulls are composed primarily of cellulosic materials with small amounts of lignin and phenolics.[34] Cottonseed, which was present in the source material used in this study, can contain nearly 30 wt % protein.[35] Manures such as broiler litter consists of a complex mixture of sterol, amino acid, and N-heterocyclic functional groups,[36] fermentation products such as volatile fatty acids and sulfides[37] and cellulose components of bedding material that account for 20−30% of broiler litter investigated in this study.[15]

Steam activation of 350BL caused a nearly vertical downward shift indicative of an increase in aromaticity. Indeed, the BET surface area of 350ABL is more than 5-fold greater than that of 350BL (Table 2). On the other hand, steam activation of 700BL caused a horizontal shift to the right with a slope of nearly zero, suggesting that steam activation resulted in an increase in oxygen functional groups, rather than the aromaticity, of 700BL. Steam activation resulted in grouping of 350BL and 700BL, originally placed in distinct regions of the van Krevelen diagram, to a proximity within the approximate elemental ratios of char.[3] Indeed, 350ABL and 700ABL have indistinguishable BET surface areas and FTIR spectra[16] and similarly affected the heavy metal sequestration in soil.[19] Post-treatment of 350BL with 0.1 M NaOH resulted in a horizontal shift to the left with a slope of nearly zero. The result is a striking contrast to the steam activation, and indicates the removal of noncarbonized fractions rich in oxygen-containing functional groups[16] as a result of the base treatment. A previous biochar amendment study on San Joaquin soil showed a mobilization of copper[19] by the base-extractable fractions of 350BL.[16] Similar results were obtained when Suwannee River natural organic matter (SRNOM), having high carboxyl and phenol functional groups,[38] was amended to San Joaquin soil.[19] When San Joaquin soil was amended with base-350BL, copper concentration in soil interstitial water decreased to below the detection limit.[19] These observations suggest the removal of oxygen-containing functional groups as a result of

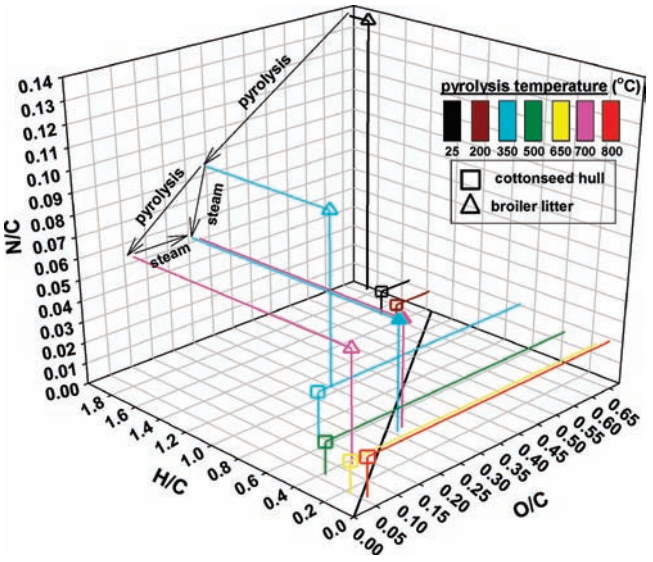

Figure 3. Three-dimensional van Krevelen diagram for broiler litter and cottonseed hull chars.

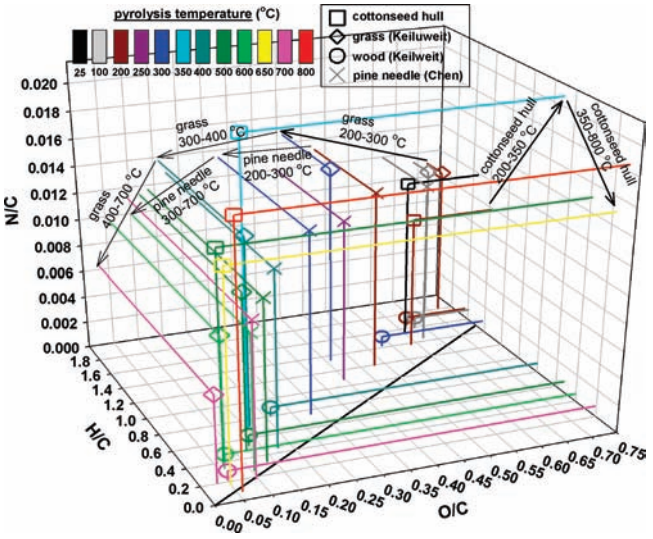

Figure 4. Three-dimensional van Krevelen diagram for cottonseed hull, pine needle, grass, and wood chars.

base treatment, and corroborate the results for 350BL and base-350BL in Figure 2. It must be noted that inherently high ash (that is high in H and O but not C) content of manure-derived carbonaceous materials[39] can impact the positioning on the van Krevelen diagram.[3]

In addition to the conventional two-dimensional van Krevelen diagram, three-dimensional plots including the N:C ratio provided additional information on the structures and transformation pathways of complex mixtures comprising coal and petroleum crude oil.[31] In Figure 3, cottonseed hull and broiler litter results in Figure 2 are extended to the three-dimensional van Krevelen plots to further elucidate the effects of pyrolysis and post-treatment on different biomass sources. The atomic N:C ratio of cottonseed hull and its pyrolysis products is significantly lower ($\leq$0.02) than that of broiler litter. Pyrolysis of broiler litter at 350 °C resulted in a sharp decrease in the N:C ratio, and further decrease was observed from 350BL to 700BL, resulting in less than half of the value relative to the source material. While steam activation reduced the N:C ratio for 350BL, the ratio for 700BL was unaffected. As a result, the N:C ratios for 700BL, 350ABL, and 700ABL are close to one another ($\approx$0.05). Base treatment of 350BL resulted in a sharp increase in the N:C ratio by more than 3-fold (Figure S3, Supporting Information). The N:C ratio of base-350BL is greater than that of the source material, and suggests the exposure of nitrogen-enriched surfaces as a result of base treatment (that removed oxygen functional groups) on partially carbonized source material.

Figure 4 presents three-dimensional van Krevelen plots for the plant-based source materials considered in Figure 2: cottonseed hull, pine needle, grass, and wood. Cottonseed hull chars, shown to have much lower N:C ratio than broiler litter in Figure 3, have among the highest N:C ratios in Figure 4. While grass and pine needle showed the N:C ratio close in range with the cottonseed hull, the N:C ratios of wood chars were significantly lower (Figure 4). For all source materials considered in Figure 4, the N:C ratio maximized near the pyrolysis temperature of 300−400 °C. The nitrogen enrichment resulted in more than 2-fold greater N:C ratio at 300 °C (maximum N:C) than 700 °C (minimum) for the grass char (Figure 4). For cottonseed hull, an increase in pyrolysis temperature from 200 to 350 °C affected N:C ratio the most, resulting in a more than 2-fold increase in the N:C ratio from 200 °C (minimum N:C) to 350 °C (maximum). Figure 4 without projections is available in Figure S4, Supporting Information.

Figure 5 presents FTIR spectra for cottonseed hull chars produced at five different pyrolysis temperatures. Peak assignments and interpretation relied extensively on Keiluweit et al.[9] where comprehensive information on characteristic vibrations of wood and grass char FTIR spectra was provided. As observed previously for wood and grass chars,[9] an increase in pyrolysis temperature from 200 to 500 °C resulted in a decrease in O−H stretching at 3200−3500 cm^{-1} attributable to hydrogen bonded hydroxyl groups. In addition, asymmetric (2935 cm^{-1}) and symmetric (2885 cm^{-1}) C−H stretchings for aliphatic functional groups decreased. Within this temperature range, symmetric C−O stretching (1030 and 1110 cm^{-1}) for the source material (cellulose, hemicellulose, and lignin) decreased (200−350 °C). Concurrently, an increase (200−350 °C) and then decrease (350−500 °C) of the following peaks were observed: carboxyl C═O (1700−1740 cm^{-1}); aromatic C═C stretching and C═O stretching of conjugated ketones and quinones (1600 cm^{-1}). At 350−650 °C, C−H bending for aromatic out-of plane deformation (750, 815, and 885 cm^{-1}) became apparent. By 800 °C, the spectrum resembles that of pure graphite, in agreement with progressive upward shift resulting from low-energy electron excitations of condensed aromatic structures.[9] A sharp increase in aromatic peaks at 300−500 °C was also observed in a previous ^{13}C CPMAS NMR analysis of chars formed by pyrolysis of tobacco.[40]

Previous thermogravimetry−mass spectrometry studies on the thermal stability of char functional groups[7] allow comparison with the FTIR results (Figure 5). Carboxylic groups decomposed to CO_2 at 100−400 °C,[7] while carboxylic anhydrides and lactones decomposed at 427−657 °C.[7] The most thermally stable C−O groups were pyrone (900−1200 °C) followed by ethers, carbonylic and quinonic groups, and phenolic and hydroquinic groups.[7] Loss of oxygen functionality with increasing pyrolysis temperature results from dehydration, decarbonylation, and decarboxylation reactions leading to condensation and the growth of aromatic structures.[7]

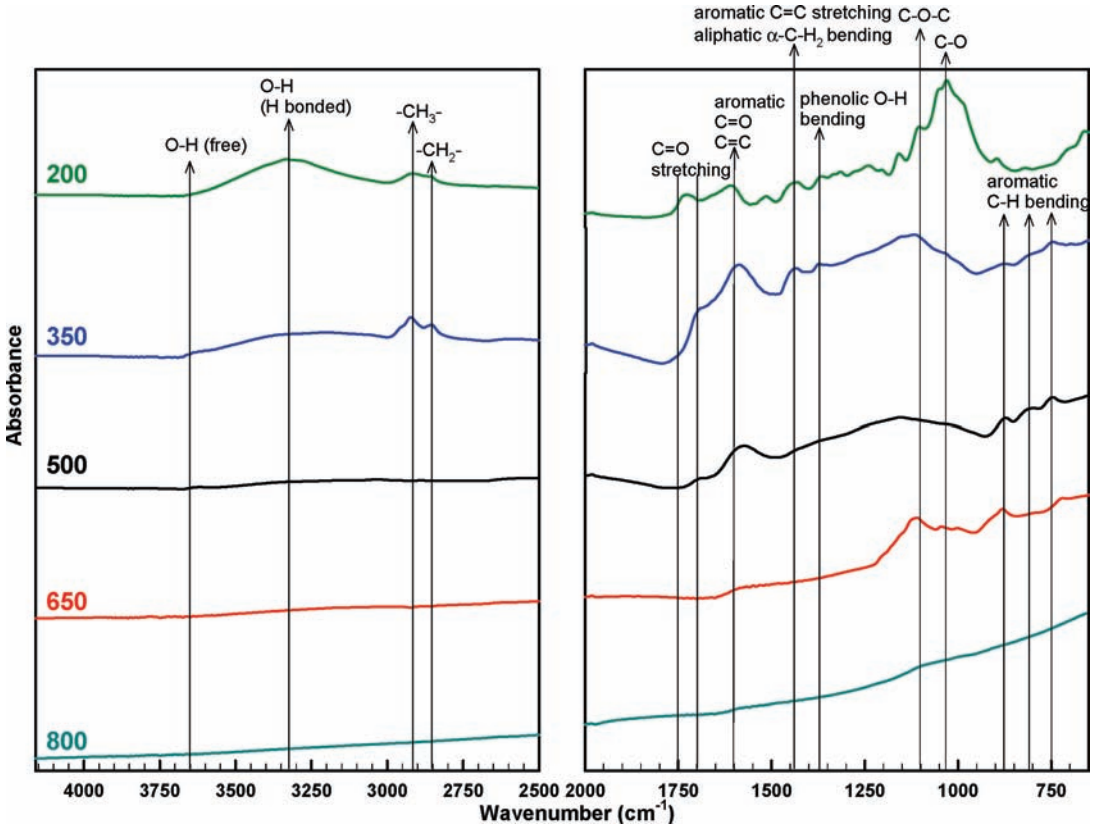

Figure 5. FTIR spectra of cottonseed hull biochars.

Role of Pyrolysis Temperature on Heavy Metal Sequestration Ability of Biochar. Figure 6 presents soluble Pb^{II}, Cd^{II}, Cu^{II}, and Ni^{II} concentrations after 48 h equilibration of Norfolk soil (20 g soil L^{-1} in SRW) amended with 10% (g biochar g^{-1} soil) CH350, CH500, CH650, CH800, PS800 and 700BL. Acidic activated carbon PS800 and basic manure biochar 700BL were employed as model carbonaceous materials that showed a particular effectiveness for heavy metal sequestration in previous studies.[14,19] Values in Figure 6 are given as mean ± SD of duplicate experiments in which Pb^{II}, Cd^{II}, Cu^{II}, and Ni^{II} were added together to each reactor for the final concentration of 300 μM for each metal (i.e., each reactor contained 1.2 mM total added metals at t_0). For all metals considered, CH350 was most effective in lowering soluble concentrations (except for PS800 and 700BL for lead, Figure 6). Equilibrium copper concentration increased in the following order: CH350 ≈ 700BL < PS800 < CH500 ≈ CH650 ≪ CH800 < soil-only (Figure 6a). Equilibrium nickel concentration increased in the following order: CH350 ≪ 700BL < PS800 < CH500 ≈ CH650 ≈ CH800 ≈ soil-only (Figure 6b). The trend observed for cadmium is similar to that for nickel, except for the greater effectiveness of 700BL (Figure 6c). Equilibrium lead concentration increased in the following order: 700BL ≈ PS800 < CH350 ≈ CH500 ≈ CH650 < CH800 ≪ soil-only (Figure 6d). Total concentration of soluble metal ions in soil interstitial waters ($[Pb^{II}] + [Cd^{II}] + [Cu^{II}] + [Ni^{II}]$) increased in the following order: CH350 < 700BL < PS800 < CH500 ≈ CH650 < CH800 < soil-only (Figure 6e). The observed trend for the total concentration correlates with the trends for nickel and cadmium having the highest equilibrium concentrations (Figure 6b,c).

Figure 6f provides pH of soil suspensions after 48 h preequilibration of amended soils in SRW (t_0 shown as squares in Figure 6f), and subsequent 48 h equilibration following the addition of Pb^{II}, Cd^{II}, Cu^{II}, and Ni^{II} (t_{48} shown as triangles in Figure 6f). The following additional values were obtained from Table 1 and plotted in Figure 6f: pH (crosses) and pH_{pzc} (horizontal lines) of cottonseed hull chars.

Except for CH800, the addition of cottonseed hull chars shifted the pH of acidic Norfolk soil (pH 5.6) to neutral (pH 7.1 for CH350) and alkaline ranges (pH 8.4 for CH500 and pH 8.2 for CH650). The addition of 700BL and PS800 resulted in significant pH increase and decrease, respectively, as reported previously.[14,19] The pH decrease as a result of equilibration (48 h) with added heavy metals (Figure 6f) has been observed previously.[14,19,41] The pH_{pzc} (Table 1) of CH500, CH650, and CH800 are significantly above pH of amended soil prior to the metal addition (pHt_0, squares in Figure 6f). In particular, pH_{pzc} of CH800 is more than 4.0 pH unit above pHt_0. In contrast, pH_{pzc} of CH350 nearly coincided with pHt_0 of 7.0. Therefore, electrostatic interactions between cationic metal species and negatively charged surfaces are expected to be significantly greater for the soil amended with CH350, in comparison to CH500, CH650, and CH800. In addition to pH_{pzc}, an increase in the following parameters of cottonseed hull chars resulted in a greater ability to retain heavy metals in Norfolk soil: VM (Figure 1d), O/C (Figure 2), and N/C (Figure 4). On the other hand, no clear correlation was observed with BET surface area, fixed C, ash content, or pH of chars. The results suggest that surface functional groups of biochars (which govern pH_{pzc} and VM and oxygen contents) control their ability to retain heavy metals in Norfolk soil.

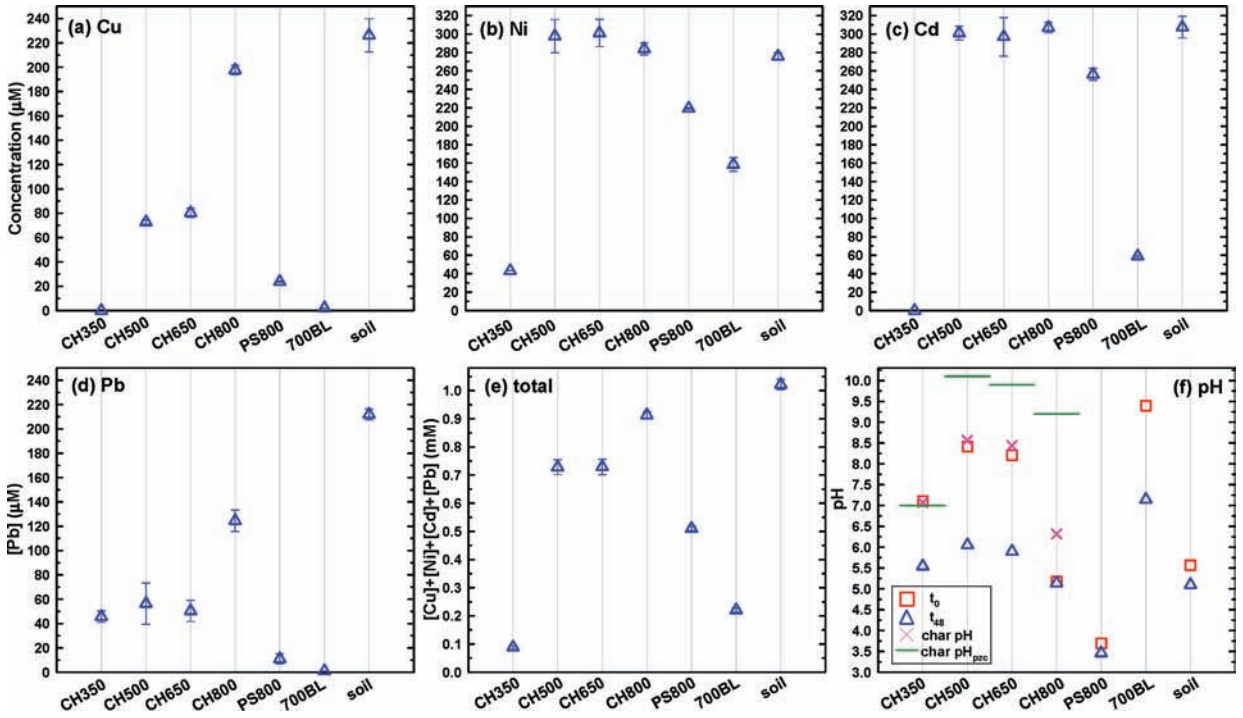

Figure 6. Concentrations of (a) Cu^{II}, (b) Ni^{II}, (c) Cd^{II}, and (d) Pb^{II} (300 μM each added together at t_0) remaining in solution after 48 h equilibration with Norfolk soil (20 g soil L^{-1} in SRW) amended with 10% char (g char g^{-1} soil). All values are shown as mean ± standard deviation for duplicate experiments. The pH before (squares) and after (triangles) 48 h equilibration with metals is provided in (f). The following values in (f) were obtained from Table 1: pH (crosses) and pH_{pzc} (horizontal lines) of chars.

Greater heavy metal retention capacity of the lower pyrolysis temperature biochar (CH350 in Figure 6) is a striking contrast to our previous observation for San Joaquin soil.[19] In San Joaquin soil, equilibrium copper concentration increased in the presence of 350BL relative to the soil-only case, while the copper concentration decreased to below detection limit in the presence of base-350BL.[19] In addition, the copper concentration increased in the presence of SRNOM containing high carboxyl and phenol functional groups that are able to complex metal ions.[38] These results suggested the mobilization of copper by complex formation with metal ion-coordinating organic fractions or competition between organic matter and metal ions for the sorption sites of biochar and soil components. Norfolk loamy sand is acidic and eroded, is low in total organic carbon content and is estimated to have 740, 250, and 10 g kg^{-1} sand, silt, and clay contents.[25] San Joaquin soil contains 40−60% clay (mainly montmorillonite)[42] and has higher pH. The carbon content of Norfolk soil is 0.6 ± 0.2 wt %, as opposed to 0.89 ± 0.05 wt % for San Joaquin soil.[14]

The total organic carbon content, cation exchange capacity, and pH of soil widely vary at different heavy metal contaminated sites[43] and scenarios (e.g., shooting range versus mining site). Norfolk soil has negligibly low copper retaining and pH buffering capacities in comparison to San Joaquin soil.[14] Contrasting results for low pyrolysis temperature biochar (from different biomass sources) amendments on Norfolk and San Joaquin soils suggest that biochars having high oxygen-containing functional groups are particularly effective for heavy metal stabilization in acidic soils with low organic carbon contents. The long-term effectiveness of biochar as a heavy metal sorbent must be considered in conjunction with the recalcitrance of biochar in soil. The stability of biochar toward microbial and abiotic degradation (that results in CO_2 release) increases as a function of pyrolysis temperature.[27] Considering the importance of oxygen functional groups for heavy metal retention (Figure 6) and the availability of oxidation methods to introduce oxygen-containing carboxyl, carbonyl, and hydroxyl groups on the char surface,[44] our future studies will report on the utility of biochars formed at high pyrolysis temperatures (650−800 °C) that are post-treated by acids and other oxidants to increase the amount of oxygen-containing surface functional groups.

■ ASSOCIATED CONTENT

Supporting Information. Proximate analysis results, determination of pH_{pzc} for cottonseed hull chars, and three-dimensional van Krevelen diagrams. This material is available free of charge via the Internet at http://pubs.acs.org.

■ AUTHOR INFORMATION

Corresponding Author

*Fax: (504) 286-4367. Phone: (504) 286-4356. E-mail: sophie.uchimiya@ars.usda.gov.

Disclaimer

Mention of trade names or commercial products in this publication is solely for the purpose of providing specific information and does not imply recommendation or endorsement by the U.S. Department of Agriculture.

■ REFERENCES

(1) Cornelissen, G.; Gustafsson, O.; Bucheli, T. D.; Jonker, M. T. O.; Koelmans, A. A.; Van Noort, P. C. M. Extensive sorption of organic compounds to black carbon, coal, and kerogen in sediments and soils:

Mechanisms and consequences for distribution, bioaccumulation, and biodegradation. *Environ. Sci. Technol.* **2005**, *39*, 6881–6895.

(2) Skjemstad, J. O.; Reicosky, D. C.; Wilts, A. R.; McGowan, J. A. Charcoal carbon in US agricultural soils. *Soil Sci. Soc. Am. J.* **2002**, *66*, 1249–1255.

(3) Hammes, K.; Smernik, R. J.; Skjemstad, J. O.; Schmidt, M. W. I. Characterisation and evaluation of reference materials for black carbon analysis using elemental composition, colour, BET surface area and C-13 NMR spectroscopy. *Appl. Geochem.* **2008**, *23*, 2113–2122.

(4) Brewer, C. E.; Schmidt-Rohr, K.; Satrio, J. A.; Brown, R. C. Characterization of biochar from fast pyrolysis and gasification systems. *Environ. Prog. Sustainable Energy* **2009**, *28*, 386–396.

(5) Steiner, C.; Teixeira, W. G.; Lehmann, J.; Nehls, T.; de Macedo, J. L. V.; Blum, W. E. H.; Zech, W. Long term effects of manure, charcoal and mineral fertilization on crop production and fertility on a highly weathered Central Amazonian upland soil. *Plant Soil* **2007**, *291*, 275–290.

(6) Antal, M. J.; Gronli, M. The art, science, and technology of charcoal production. *Ind. Eng. Chem. Res.* **2003**, *42*, 1619–1640.

(7) Bourke, J.; Manley-Harris, M.; Fushimi, C.; Dowaki, K.; Nunoura, T.; Antal, M. J. Do all carbonized charcoals have the same chemical structure? 2. A model of the chemical structure of carbonized Charcoal. *Ind. Eng. Chem. Res.* **2007**, *46*, 5954–5967.

(8) Meszaros, E.; Jakab, E.; Varhegyi, G.; Bourke, J.; Manley-Harris, M.; Nunoura, T.; Antal, M. J. Do all carbonized charcoals have the same chemical structure? 1. Implications of thermogravimetry - mass spectrometry measurements. *Ind. Eng. Chem. Res.* **2007**, *46*, 5943–5953.

(9) Keiluweit, M.; Nico, P. S.; Johnson, M. G.; Kleber, M. Dynamic molecular structure of plant biomass-derived black carbon (biochar). *Environ. Sci. Technol.* **2010**, *44*, 1247–1253.

(10) Keiluweit, M.; Kleber, M. Molecular-level interactions in soils and sediments: The role of aromatic pi-systems. *Environ. Sci. Technol.* **2009**, *43*, 3421–3429.

(11) Chen, B. L.; Zhou, D. D.; Zhu, L. Z. Transitional adsorption and partition of nonpolar and polar aromatic contaminants by biochars of pine needles with different pyrolytic temperatures. *Environ. Sci. Technol.* **2008**, *42*, 5137–5143.

(12) Chun, Y.; Sheng, G. Y.; Chiou, C. T.; Xing, B. S. Compositions and sorptive properties of crop residue-derived chars. *Environ. Sci. Technol.* **2004**, *38*, 4649–4655.

(13) Kasozi, G. N.; Zimmerman, A. R.; Nkedi-Kizza, P.; Gao, B. Catechol and humic acid sorption onto a range of laboratory-produced black carbons (biochars). *Environ. Sci. Technol.* **2010**, *44*, 6189–95.

(14) Uchimiya, M.; Klasson, K. T.; Wartelle, L. H.; Lima, I. M. Influence of soil properties on heavy metal sequestration by biochar amendment: 1. Copper sorption isotherms and the release of cations. *Chemosphere* **2011**, *82*, 1431–1437.

(15) Lima, I. M.; Boateng, A. A.; Klasson, K. T. Pyrolysis of broiler manure: Char and product gas characterization. *Ind. Eng. Chem. Res.* **2009**, *48*, 1292–1297.

(16) Uchimiya, M.; Lima, I. M.; Klasson, K. T.; Chang, S.; Wartelle, L. H.; Rodgers, J. E. Immobilization of heavy metal ions (Cu^{II}, Cd^{II}, Ni^{II}, Pb^{II}) by broiler litter-derived biochars in water and soil. *J. Agric. Food Chem.* **2010**, *58*, 5538–5544.

(17) Kappler, A., M; Benz, B.; Schink, B.; Brune, A. Electron shuttling via humic acids in microbial iron(II) reduction in freshwater sediment. *FEMS Microbiol. Ecol.* **2004**, *47*, 85–92.

(18) Klasson, K. T.; Wartelle, L. H.; Rodgers, J. E.; Lima, I. M. Copper(II) adsorption by activated carbons from pecan shells: Effect of oxygen level during activation. *Ind. Crop. Prod.* **2009**, *30*, 72–77.

(19) Uchimiya, M.; Lima, I. M.; Klasson, K. T.; Wartelle, L. H. Contaminant immobilization and nutrient release by biochar soil amendment: Roles of natural organic matter. *Chemosphere* **2010**, *80*, 935–940.

(20) D5142. *Standard Test Methods for Proximate Analysis of the Analysis Sample of Coal and Coke by Instrumental Procedures*; American Society for Testing and Materials,:West Conshohocken, PA, 2009.

(21) Yang, Y. N.; Chun, Y.; Sheng, G. Y.; Huang, M. S. pH-dependence of pesticide adsorption by wheat-residue-derived black carbon. *Langmuir* **2004**, *20*, 6736–6741.

(22) Dastgheib, S. A.; Karanfil, T.; Cheng, W. Tailoring activated carbons for enhanced removal of naturalorganic matter from natural waters. *Carbon* **2004**, *42*, 547–557.

(23) Hooper, K.; Iskander, M.; Sivia, G.; Hussein, F.; Hsu, J.; Deguzman, M.; Odion, Z.; Ilejay, Z.; Sy, F.; Petreas, M.; Simmons, B. Toxicity characteristic leaching procedure fails to extract oxoanion-forming elements that are extracted by municipal solid waste leachates. *Environ. Sci. Technol.* **1998**, *32*, 3825–3830.

(24) Kieber, R. J.; Skrabal, S. A.; Smith, C.; Willey, J. D. Redox speciation of copper in rainwater: Temporal variability and atmospheric deposition. *Environ. Sci. Technol.* **2004**, *38*, 3587–3594.

(25) Novak, J. M.; Bauer, P. J.; Hunt, P. G. Carbon dynamics under long-term conservation and disk tillage management in a Norfolk loamy sand. *Soil Sci. Soc. Am. J.* **2007**, *71*, 453–456.

(26) Spokas, K. A.; Koskinen, W. C.; Baker, J. M.; Reicosky, D. C. Impacts of woodchip biochar additions on greenhouse gas production and sorption/degradation of two herbicides in a Minnesota soil. *Chemosphere* **2009**, *77*, 574–581.

(27) Zimmerman, A. R. Abiotic and microbial oxidation of laboratory-produced black carbon (biochar). *Environ. Sci. Technol.* **2010**, *44*, 1295–1301.

(28) Kamath, S. R.; Proctor, A. Silica gel from rice hull ash: Preparation and characterization. *Cereal Chem.* **1998**, *75*, 484–487.

(29) Pignatello, J. J.; Kwon, S.; Lu, Y. F. Effect of natural organic substances on the surface and adsorptive properties of environmental black carbon (char): Attenuation of surface activity by humic and fulvic acids. *Environ. Sci. Technol.* **2006**, *40*, 7757–7763.

(30) Visser, S. A. Application of van Krevelen's graphical-statistical method for the study of aquatic humic material. *Environ. Sci. Technol.* **1983**, *17*, 412–417.

(31) Wu, Z. G.; Rodgers, R. P.; Marshall, A. G. Two- and three-dimensional van Krevelen diagrams: A graphical analysis complementary to the Kendrick mass plot for sorting elemental compositions of complex organic mixtures based on ultrahigh-resolution broadband Fourier transform ion cyclotron resonance mass measurements. *Anal. Chem.* **2004**, *76*, 2511–2516.

(32) Kim, S.; Kramer, R. W.; Hatcher, P. G. Graphical method for analysis of ultrahigh-resolution broadband mass spectra of natural organic matter, the van Krevelen diagram. *Anal. Chem.* **2003**, *75*, 5336–5344.

(33) Hammes, K.; Schmidt, M. W. I.; Smernik, R. J.; Currie, L. A.; Ball, W. P.; Nguyen, T. H.; Louchouarn, P.; Houel, S.; Gustafsson, O.; Elmquist, M.; Cornelissen, G.; Skjemstad, J. O.; Masiello, C. A.; Song, J.; Peng, P.; Mitra, S.; Dunn, J. C.; Hatcher, P. G.; Hockaday, W. C.; Smith, D. M.; Hartkopf-Froeder, C.; Boehmer, A.; Luer, B.; Huebert, B. J.; Amelung, W.; Brodowski, S.; Huang, L.; Zhang, W.; Gschwend, P. M.; Flores-Cervantes, D. X.; Largeau, C.; Rouzaud, J. N.; Rumpel, C.; Guggenberger, G.; Kaiser, K.; Rodionov, A.; Gonzalez-Vila, F. J.; Gonzalez-Perez, J. A.; de la Rosa, J. M.; Manning, D. A. C.; Lopez-Capel, E.; Ding, L. Comparison of quantification methods to measure fire-derived (black/elemental) carbon in soils and sediments using reference materials from soil, water, sediment and the atmosphere. *Global Biogeochem. Cycles* **2007**, *21*, GB3016.

(34) Himmelsbach, D. S.; Hellgeth, J. W.; McAlister, D. D. Development and use of an attenuated total reflectance/fourier transform infrared (ATR/FT-IR) spectral database to identify foreign matter in cotton. *J. Agric. Food Chem.* **2006**, *54*, 7405–7412.

(35) Berberich, S. A.; Ream, J. E.; Jackson, T. L.; Wood, R.; Stipanovic, R.; Harvey, P.; Patzer, S.; Fuchs, R. L. The composition of insect-protected cottonseed is equivalent to that of conventional cottonseed. *J. Agric. Food Chem.* **1996**, *44*, 365–371.

(36) Schnitzer, M. I.; Monreal, C. M.; Facey, G. A.; Fransham, P. B. The conversion of chicken manure to biooil by fast pyrolysis I. Analyses of chicken manure, biooils and char by C-13 and H-1 NMR and FTIR spectrophotometry. *J. Environ. Sci. Health B* **2007**, *42*, 71–77.

(37) Miller, D. N.; Varel, V. H. An in vitro study of manure composition on the biochemical origins, composition, and accumulation of odorous compounds in cattle feedlots. *J. Anim. Sci.* **2002**, *80*, 2214–2222.

(38) Rakshit, S.; Uchimiya, M.; Sposito, G. Iron(III) bioreduction in soil in the presence of added humic substances. *Soil Sci. Soc. Am. J.* **2009**, *73*, 65–71.

(39) Lima, I. M.; Marshall, W. E. Granular activated carbons from broiler manure: physical, chemical and adsorptive properties. *Bioresour. Technol.* **2005**, *96*, 699–706.

(40) Sharma, R. K.; Wooten, J. B.; Baliga, V. L.; Martoglio-Smith, P. A.; Hajaligol, M. R. Characterization of char from the pyrolysis of tobacco. *J. Agric. Food Chem.* **2002**, *50*, 771–83.

(41) Yu, S.; He, Z. L.; Huang, C. Y.; Chen, G. C.; Calvert, D. V. Adsorption-desorption behavior of copper at contaminated levels in red soils from China. *J. Environ. Qual.* **2002**, *31*, 1129–1136.

(42) Schoups, G.; Hopmans, J. W.; Young, C. A.; Vrugt, J. A.; Wallender, W. W.; Tanji, K. K.; Panday, S. Sustainability of irrigated agriculture in the San Joaquin Valley, California. *Proc. Natl. Acad. Sci. U. S.A.* **2005**, *102*, 15352–15356.

(43) Bannon, D. I.; Drexler, J. W.; Fent, G. M.; Casteel, S. W.; Hunter, P. J.; Brattin, W. J.; Major, M. A. Evaluation of small arms range soils for metal contamination and lead bioavailability. *Environ. Sci. Technol.* **2009**, *43*, 9071–9076.

(44) Cho, H.-H.; Wepasnick, K.; Smith, B. A.; Bangash, F. K.; Fairbrother, D. H.; Ball, W. P. Sorption of aqueous Zn[II] and Cd[II] by multiwall carbon nanotubes: The relative roles of oxygen-containing functional groups and graphenic carbon. *Langmuir* **2010**, *26*, 967–981.